Role of TXNIP/NLRP3 in sepsis-induced myocardial dysfunction

CHUN YANG[1], WAN XIA[2], XIAOLIN LIU[2], JIAN LIN[2] and AIPING WU[2]

[1]Department of Emergency Medicine, Tongde Hospital of Zhejiang Province, Hangzhou, Zhejiang 310012; [2]Department of Rehabilitation Medicine, Zhejiang Hospital, Hangzhou, Zhejiang 310013, P.R. China

Received November 28, 2018; Accepted May 8, 2019

DOI: 10.3892/ijmm.2019.4232

Abstract. Myocardial injury is one of the main symptoms of sepsis. However, the mechanisms underlying sepsis-induced myocardial dysfunction remain unclear. In the present study, the concentration of cardiac troponin T (CTnT) in serum was measured using an enzyme-linked immunosorbent assay kit. The levels of interleukin (IL)-1β and IL-18 were assessed by reverse transcription-quantitative polymerase chain reaction (RT-qPCR) analysis and the level of malondialdehyde (MDA) was determined using a corresponding kit. Myocardial pathology was analyzed via hematoxylin and eosin staining. RT-qPCR analysis and western blotting and/or immunohistochemistry were used to quantify the expression levels of thioredoxin-interacting protein (TNXIP), NOD-like receptor pyrin domain containing 3 (NLRP3), cleaved caspase-1, caspase-1, catalase and manganese-superoxide dismutase (MnSOD). The viability of cells was determined using a cell counting kit-8. Apoptosis and reactive oxygen species (ROS) were examined using flow cytometry. Models of sepsis-induced myocardial injury were successfully established; evidence included increases in the levels of CTnT, IL-1β, IL-18 and MDA and myocardial tissue damage *in vivo*, and decreased cell viability and improvements in IL-1β and IL-18 *in vitro*. The levels of TXNIP, NLRP3 and cleaved caspase-1 were upregulated in the sepsis models. Small interfering RNA targeting TNXNIP (siTXNIP) increased cell viability, reduced the apoptotic rate and attenuated the release of IL-1β and IL-18. The levels of TXNIP, NLRP3 and cleaved caspase-1 and production of ROS were suppressed by siTXNIP, accompanied by increases in catalase and MnSOD. TXNIP/NLRP3 serves an important role in the development of sepsis-induced myocardial damage.

Correspondence to: Dr Aiping Wu, Department of Rehabilitation Medicine, Zhejiang Hospital, 12 Lingyin Road, Hangzhou, Zhejiang 310013, P.R. China
E-mail: waiping_apwu@163.com

Key words: sepsis, myocardial dysfunction, thioredoxin-interacting protein, NOD-like receptor pyrin domain containing 3

Introduction

Sepsis refers to the systemic inflammatory response syndrome caused by the invasion of pathogenic microorganisms; their toxins and metabolites invade into the circulating blood, activating human cells and the humoral immune system to produce various cytokines and endogenous mediators (1). Myocardial tissue is a common target organ involved in the course of sepsis, and myocardial tissue damage is the starting point of multiple organ dysfunction syndromes (2). Numerous clinical and animal studies have confirmed the presence of cardiomyocyte inhibition in sepsis, which is one of the factors contributing to cardiac insufficiency and hemodynamic instability (3). Cardiac troponin T (CTnT) is a sensitive indicator of myocardial damage, and 31-85% of patients have severely elevated serum troponin (4). However, there is no clear understanding of the mechanism underlying the effects of sepsis on myocardial injury.

The overactivation of apoptosis is an important pathological feature of tissue damage during sepsis (5), however, the specific mechanism underlying the tissue damage and excessive apoptosis of cells remains to be fully elucidated. The close association between the oxidative stress response and inflammation has received increasing attention in recent years, and the effects of inflammation on mitochondrial function lead to an increase in the production of reactive oxygen species (ROS), which in turn causes tissue damage through the activation of oxidative stress (6).

The molecular mechanisms responsible for the inflammatory reactions caused by inflammatory cytokines, leading to the inhibition of cardiac function, have been investigated (7), however, the specific molecular mechanisms remain unclear. Studies have shown that inflammasomes are involved in the damage of myocardial tissue (8). It is known that the NO-like-binding domain (NOD)-like receptor protein 3 (NLRP3) inflammasome usually consists of three main components, including NLRP3, apoptosis-associated speck-like protein (ASC) and aspartate proteolysis, which is a protein complex composed of cysteinylaspartate-specific proteases-1 (caspase-1) protein (9). It was found that thioredoxin-interacting protein (TXNIP) directly activated caspase-1 and then activated caspase-1, cleaved caspase-1, cleaved pro-interleukin (IL)-1β and pro-IL-18. Following cutting, the cells released physiologically active IL-1β and IL-18, eventually producing an inflammatory response (10). In addition, ROS have been identified as one of the mediators that activates the NLRP3 inflammasome (11).

Oxidative stress refers to the imbalance between oxidation and anti-oxidation, including the excessive production of ROS (12) in the body. Malondialdehyde (MDA) is a product of lipid oxidation and is responsible for the formation of ROS and the extent of oxidative damage (13). Intracellular ROS are cleared mainly through antioxidant enzyme substances, including superoxide dismutase (SOD) and catalase. SOD has three subtypes, Cu/ZnSOD, FeSOD and MnSOD, among which MnSOD accounts for 70% of the total SOD in the heart and up to 90% in cardiomyocytes (14). The expression of MnSOD in mitochondria regulates the production of O_2^- during oxidative phosphorylation, thus, MnSOD serves a key role in ROS (15).

The present study established a rat and cell sepsis model and observed changes to myocardial tissue and cells by detecting changes in CTnT, inflammatory factors, MAD, SOD and NLRP3/TXNIP in order to provide a promising therapeutic target for the myocardial protection of clinical sepsis.

Materials and methods

Animals. Twelve adult male Sprague-Dawley (SD) rats (8-weeks old, weighing 180-250 g) were obtained from the Shanghai SLAC Laboratory Animal Co., Ltd.; the rats were housed in groups of three per cage with food and water available *ad libitum*, and were maintained in controlled room temperature (22±2˚C) and humidity (60-80%) under a 12 h/12 h light/dark cycle. All animal protocols were approved by Zhejiang University Animal Committee (Zhejiang, China).

Reagents. Lipopolysaccharide (LPS) was purchased from Sigma-Aldrich; Merck KGaA (Darmstadt, Germany). CTnT enzyme-linked immunosorbent assay (ELISA) kits were purchased from R&D systems, Inc. (Minneapolis, MN, USA). MDA levels were determined using the TBA method (Jian Cheng Bioengineering Institute, Nanjing, China). Small interfering RNA targeting TNXIP (siTNXIP) and negative control (TNXIP-NC) were purchased from GenePharma (Shanghai, China).

LPS injection of rats and groups. LPS was dissolved in sterile physiological saline (0.9% NaCl) at a concentration of 1 mg/ml. The rats were injected intraperitoneally with 10 mg LPS/kg. The treatment was performed respectively for 6, 12 and 24 h for pathological analysis. The control group was injected with the same volume of physiological saline in the same manner.

MDA measurement via the TBA method. All rats were sacrificed by intraperitoneal injection of sodium pentobarbital (200 mg/kg) following LPS treatment for 6, 12 and 24 h. The rats in the control group were sacrificed using the same method. The absence of sounds of breathing and heartbeat, namely respiratory arrest and cardiac arrest, through a stethoscope confirmed death of the rats. Heart tissues (0.5 g) from the same position were removed from the rats in the four groups and homogenized with physiological saline. Subsequently, 0.2 ml homogenate with 0.2 ml 8.1% SOS, 1.5 ml 20% acetic acid and 1.5 ml 0.8% TBA aqueous solution was placed in a lidded glass test tube and then diluted to 4 ml with triple-distilled water, and placed in a water bath for 60 min at 95˚C. The samples were removed and cooled to room temperature, and 1 ml distilled water and 5 ml n-butanol pyridine solution were added to the samples, following which the mixture was shaken for 15 min and separated at 3,000 x g for 15 min at room temperature. The n-butanol phase at 532 μm was measured for colorimetric densities. The value of fluorescence was calculated by comparing with standards prepared from 1,1,3,3-tetraethoxypropane (cat. no. T9889, Sigma-Aldrich; Merck KGaA).

Hematoxylin and eosin staining. Myocardial tissue was removed and the samples were fixed with 10% paraformaldehyde solution for >48 h, following which they were routinely dehydrated and paraffin-embedded to prepare 5-μm tissue sections. The sections were heated in an incubator at 68˚C for 1-2 h, and were then placed in xylene for dewaxing three times for 30 min. The sections were then placed in 100, 95, 85 and 75% gradient alcohol for hydration for 5 min. Following washing the sections for 2 min in tap water, the sections were stained with hematoxylin for 10 min and with eosin for 30 sec at room temperature. The sections were then infiltrated with xylene for 5 sec, and the neutral gum was sealed and observed under a light microscope (BX51, Olympus Corporation, Tokyo, Japan).

Immunohistochemical analyses. The tissue samples obtained from all rats for histological and immunohistochemical analyses were fixed in 10% formalin solution and embedded in paraffin, according to conventional histological methods. The paraffin-embedded tissue samples were cut into 5-μm thick sections and the immunohistochemical expression of TXNIP and NLRP3 in tissue sections were determined using avidin-biotin-peroxidase complex. The tissue sections were deparaffinized, rehydrated and treated with 3% H_2O_2 to block endogenous peroxidase activity. Subsequently, the sections were incubated in citrate buffer (0.1 M, pH 6.0) in a microwave (800 W, 10 min) and washed with a phosphate buffer solution (PBS; 0.1 M, pH 7.2). The sections were then incubated in a blocking buffer (5% bovine serum albumin; cat. no. B2064; Sigma-Aldrich; Merck KGaA) for 10 min at room temperature., washed with PBS and incubated with anti-TXNIP (cat. no. ab231966, dilution 1:500, Abcam, Cambridge, MA, USA) and anti-NLRP3 (cat. no. ab214185, dilution 1:500, Abcam) antibodies for 1 h at room temperature and washed again with PBS. The sections were then incubated with horseradish peroxidase-conjugated goat anti-rabbit immunoglobulin G (1:250; cat. no. sc-2004; Santa Cruz Biotechnology, Inc.) for 30 min at room temperature. Finally, the sections were washed again and treated with a 3,3-diaminobenzidine substrate system (Thermo Fisher Scientific, Inc., Waltham, MA, USA). Negative control (NC) samples were used to determine specific TXNIP and NLRP3 immunoreactivity. The number of positive microvessels in each section was counted in 10 microscopic fields (magnifications, x100 and x200) under a light microscope (BX51, Olympus Corporation).

H9C2 cells and culture. The H9C2 cell line was purchased from American Type Culture Collection (Rockville, MD, USA); the cells were cultured in Dulbecco's modified Eagle's medium (DMEM; Gibco; Thermo Fisher Scientific, Inc.)

supplemented with 10% fetal bovine serum (FBS; Gibco; Thermo Fisher Scientific, Inc.) and 100 μg/ml penicillin and 100 μg/ml streptomycin (Gibco; Thermo Fisher Scientific, Inc.) at 37˚C in a humidified atmosphere at 5% CO_2 in air. Subsequently, $2x10^5$ cells were seeded onto culture plates and cultured in medium with LPS (1, 10, 20 and 50 μg/ml) for 24 h at 37˚C. siTXNIP was added into the culture medium for transfection 24 h prior to the LPS (20 μg/ml) treatment. Following incubation, the cells were collected for the analysis of cellular viability, mRNA and protein expression, apoptosis and ROS.

Transfection. To investigate the role of TXNIP in sepsis-induced myocardial dysfunction, the H9C2 cells were divided into five groups, as follows: Control group, LPS group (cells were treated with LPS), NC+LPS group (cells were transfected with empty vector and treated with LPS), siTXNIP+LPS group (cells were transfected with siTXNIP and treated with LPS) and siTXNIP group (cells were transfected with siTXNIP). Lipofectamine™ 3000 (LFN) transfection (Thermo Fisher Scientific, Inc.) was performed according to the manufacturer's instructions. In brief, the lipid complex was prepared by combining the reagent of 4 μl LFN Plus with 2 μg of plasmid DNA and then suspended in 1 ml serum-free medium and incubated at room temperature for 15 min. The solution was then mixed with 40 μl of LFN in serum-free medium and incubated at room temperature for 15 min. The lipid compounds were diluted in serum-free medium to produce a 5-ml volume of the required concentration, and the cells were incubated at 37˚C with 5% CO_2 for 24 h.

Cell viability assay. Following transfection of the H9C2 cells with or without siTXNIP prior to LPS treatment, 10 μl of cell counting kit (CCK)-8 solution was added to the wells and the cell were incubated at 37˚C for 2 h tin an incubator with 5% CO_2 in the dark. Subsequently, the OD value in each well from different cell groups at an absorbance of 450 nm was determined using a microplate reader (Bio-Rad Laboratories, Inc., Hercules, CA, USA). Cell viability was detected with the CCK-8 assay kit according to the manufacturer's protocol.

Apoptosis. Following treatment of the H9C2 cells for 24 h, $1x10^6$ cells were collected and 1 ml of trypsin (trypsin) without ethylenediaminetetraacetic acid was used to digest the cells, which were shaken gently, and trypsin was removed when the wall was wet. After 1 min at room temperature, the digestion was terminated by adding DMEM (Corning) containing 10% FBS. The cells were centrifuged at 1,000 x g for 3 min at room temperature and the supernatant was removed. The cells were washed twice with pre-cooled PBS and resuspended in 1X Annexin V binding buffer. According to the Annexin V-FITC cell apoptosis detection kit (cat. no. K201-100, BioVision, Inc., Milpitas, CA, USA), the cells were stained with 1.25 μl Annexin V-FITC and 10 μl propidium iodide and measured by flow cytometry (version 10.0, FlowJo, FACSCalibur™, BD Biosciences, Franklin Lakes, NJ, USA).

ROS measurement by flow cytometry. The H9C2 cells were transfected with siTNXIP and then treated with LPS. The cells were then incubated with 2',7'-dichloro dihydrogen fluorescein diacetate ester (Beyotime Institute of Biotechnology, Shanghai, China, 5 μM) for 30 min at 37˚C. The excitation wavelength of the flow cytometry (version 10.0, FlowJo, BD Biosciences) was 480 nm and the emission wavelength was 525 nm.

Western blot analysis. The tissues and the H9C2 cells were flushed with cold PBS three times and placed on the ice with protein lysis buffer (RIPA; Cell Signaling Technology, Inc., Danvers, MA, USA) for 2 h. The samples were centrifuged at 13,500 x g for 30 min at 4˚C and the supernatants were extracted. The concentration of protein was determined using a BCA protein assay kit (Bio-Rad Laboratories, Inc.). Subsequently, SDS-PAGE with 10% running gels was used to separate the proteins (at least 40 μg), which were then transferred onto a polyvinylidene fluoride membrane (Bio-Rad Laboratories, Inc.). To block the nonspecific signals, the membrane was incubated with 5% non-fat milk for at least 2 h at room temperature. The proteins were then incubated with primary antibody overnight at 4˚C and then washed with 5% bovine serum albumin (Gibco; Thermo Fisher Scientific, Inc.) in PBS/0.1% Tween-20 and incubated with secondary antibodies (cat. nos. sc-2004 and sc-2005, 1:2,000; Santa Cruz Biotechnology, Inc. Dallas, TX, USA) for 1 h at room temperature. The protein bands were developed with developer (EZ-ECL kit; Biological Industries) and protein quantity was analyzed using ImageJ software (version 5.0; Bio-Rad Laboratories). The antibodies used were as follows: Anti-GAPDH (mouse; cat. no. sc-47724, 1:1,000; Santa Cruz Biotechnology, Inc.), anti-TXNIP (rabbit, cat. no. ab210826, 1:1,000, Abcam), anti-NLRP3 (rabbit, cat. no. ab214185, 1:1,000, Abcam), anti-caspase-1 (rabbit, cat. no. ab1872, 1:1,000, Abcam), and anti-cleaved caspase-1 (rabbit, cat. no. ab25901, 1:1,000, Abcam), anti-catalase (rabbit, cat. no. ab16731, 1:1,000, Abcam), anti-MnSOD (rabbit, cat. no. ab13533, 1:1,000, Abcam) and secondary antibodies (cat. nos. sc-2004 and sc-2005, 1:2,000; Santa Cruz Biotechnology, Inc.).

RNA isolation and reverse transcription-quantitative polymerase chain reaction (RT-qPCR) analysis. According to the program provided by the manufacturer, total RNA of the tissues and H9C2 cells was extracted using TRIzol reagent (Invitrogen; Thermo Fisher Scientific, Inc.). Chloroform (Sigma Aldrich; Merck KGaA) was added to the tube and incubated at room temperature for 5 min and centrifuged at 14,000 x g for 20 min at 4˚C. The supernatant was transferred to a new tube and isopropanol was added. The aqueous phase was centrifuged at 14,000 x g for 20 min at 4˚C. The precipitate was washed with 70% ethanol and suspended again in water treated with 0.1% diethyl carbamate. The purity and concentration of the RNA was assessed using the NanoDrop ND-1000 spectrophotometer (NanoDrop Technologies; Thermo Fisher Scientific, Inc.), and the absorbance was read at 260 and 280 nm. According to the program provided by the manufacturer (Thermo Fisher Scientific, Inc.), a reverse transcription cDNA kit was used to reverse transcribe 1 μg total RNA for the synthesis of cDNA (at 42˚C for 60 min, at 70˚C for 5 min, and preserved at 4˚C). SYBR-Green PCR Master mix (Roche Diagnostics, Basel, Switzerland) was used to perform the qPCR experiment using the Opticon real-time PCR detection system

Table I. Primers for reverse transcription-quantitative polymerase chain reaction.

Gene	Forward (5'-3')	Reverse (5'-3')
IL-1β (mouse)	TCGCCAGTGAAATGATGGCTTA	GTCCATGGCCACAACAACTGA
IL-18 (mouse)	GACCTTCCAGATCGCTTCCTC	GATGCAATTGTCTTCTACTGGTTC
IL-1β (human)	TGCAGAGTTCCCCAACTGGTACATC	GTGCTGCCTAATGTCCCCTTGAATC
IL-18 (human)	ATCAACCTCAGACCTTCCAG	GCATTATCTCTACAGTCAG
TXNIP (human)	GCCACACTTACCTTGCCAAT	TTGGATCCAGGAACGCTAAC
MnSOD (human)	CAGACCTGCCTTACGACTATGG	CTCGGTGGCGTTGAGATTGTT
Catalase (human)	CGTGCTGAATGAGGAACAGA	AGTCAGGGTGGACCTCAGTG
GAPDH (mouse)	GCACCGTCAAGCTGAGAAC	TGGTGAAGACGCCAGTGGA
GAPDH (human)	AGGTCGGTGTGAACGGATTTG	GGGGTCGTTGATGGCAACA

IL, interleukin; TXNIP, thioredoxin-interacting protein; MnSOD, manganese-superoxide dismutase.

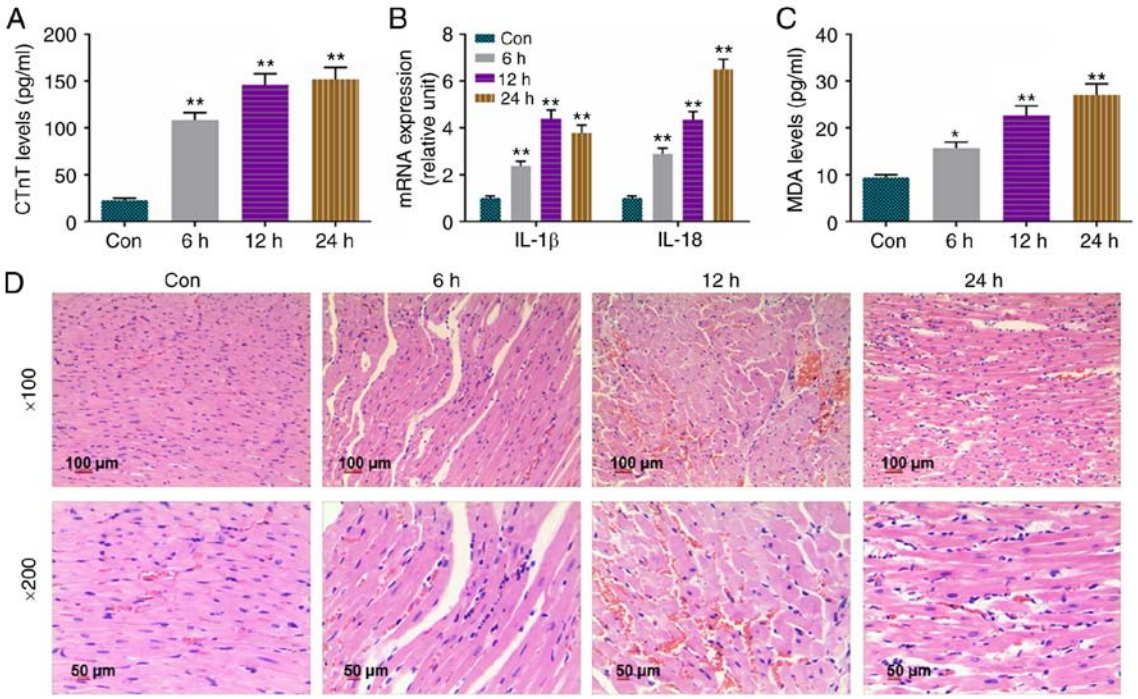

Figure 1. Levels of CThT, IL-1β, IL-18 and MDA are increased and pathology is altered in sepsis-induced myocardial injury in rats. (A) Levels of CThT were determined by enzyme-linked immunosorbent assay. (B) Reverse transcription-quantitative polymerase chain reaction analysis was used to determine the mRNA levels of IL-1β and IL-18. (C) Levels of MDA were identified by thiobarbituric acid reaction colorimetry. (D) Pathological changes of myocardial tissue were analyzed by hematoxylin and eosin staining. *P<0.05 and **P<0.01 vs. Con. CThT, cardiac troponin T; IL, interleukin; MDA, malondialdehyde; Con, control.

(ABI 7500; Thermo Fisher Scientific, Inc.). The thermocycling conditions were as follows: 40 cycles at 95˚C for 15 sec, at 60˚C for 1 min). The relative mRNA quantity was determined using the comparative cycle threshold ($2^{-\Delta\Delta Cq}$) method (16). The expression of GAPDH was used for normalization. The primer sequences used for RT-qPCR are listed in Table I.

Statistical analysis. Values are presented as the mean ± standard error of the mean. GraphPad Prism 5 (GraphPad Software, Inc., La Jolla, CA, USA) was used to analyze the values. One-way analysis of variance followed by Turkey's post hoc test was applied to analyze differences among the experimental groups. P<0.05 was considered to indicate a statistically significant difference.

Results

Levels of CTnT, IL-1β, IL-18 and MDA are increased and pathology is altered in sepsis-induced myocardial injury rats. The present study determined CTnT levels in the serum of control rats and in septic rats treated for 6, 12 and 24 h. Quantification of CTnT levels was achieved using the ELISA method, and the results showed that the levels of CTnT were significantly higher in the 6, 12 and 24 h groups, compared with than that in the Con group (Fig. 1A). Detection by RT-qPCR analysis (Fig. 1B) revealed that the expression levels of IL-1β and IL-18 were increased in the 6, 12 and 24 h groups, compared with those in the Con group. MDA, a byproduct of unsaturated fatty acid oxidation, was measured

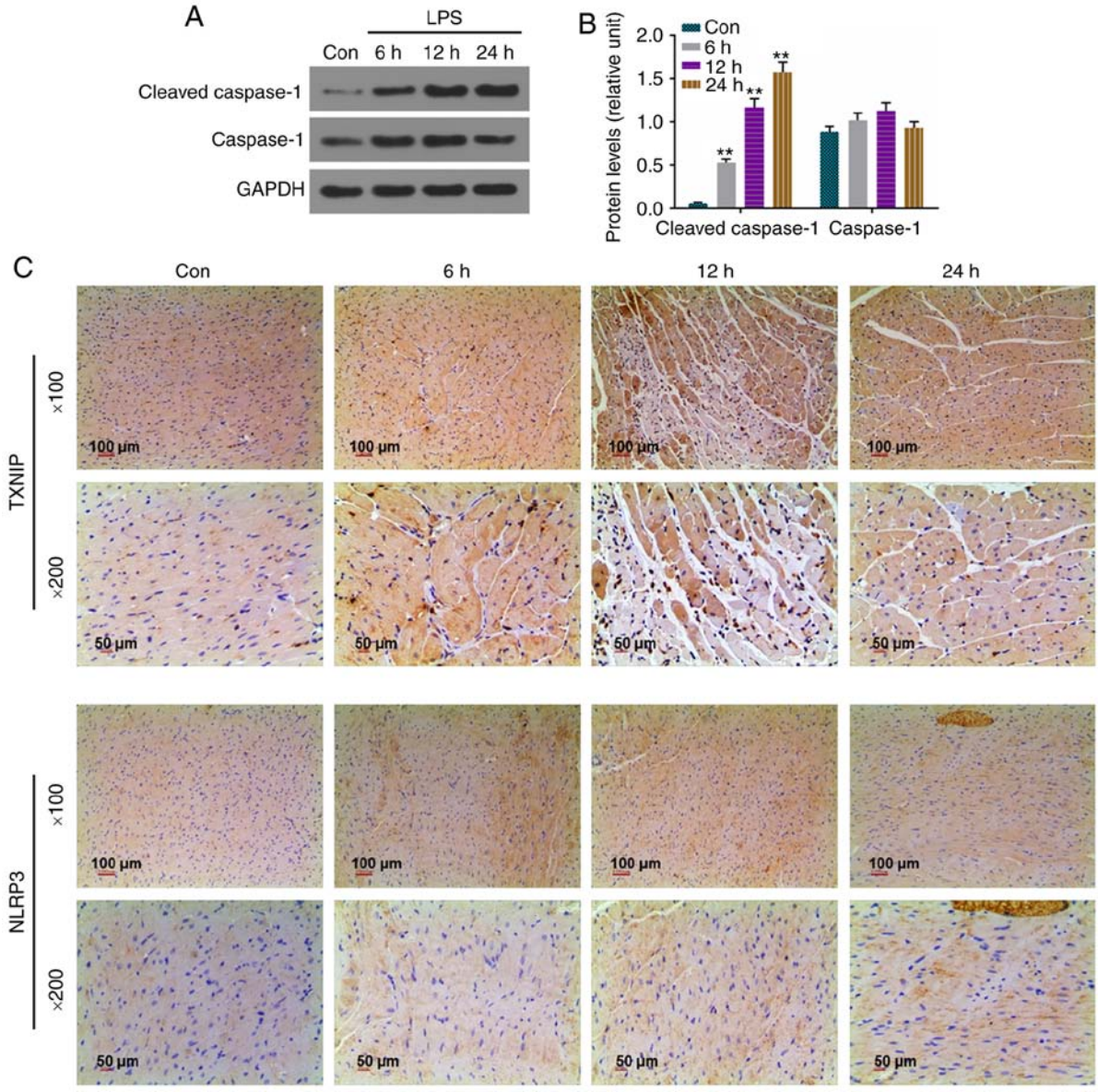

Figure 2. Protein levels of cleaved caspase-1 are upregulated and TXNIP and NLRP3 staining is strong in sepsis-induced myocardial injury in rats. (A) Protein levels of cleaved caspase-1 and caspase-1 were assessed by western blotting. (B) Relative levels of proteins were determined with GAPDH for normalization. (C) TXNIP and NLRP3 were stained using immunochemistry. **P<0.01 vs. Con. TXNIP, thioredoxin-interacting protein; NLRP3, NOD-like receptor pyrin domain containing 3; LPS, lipopolysaccharide; Con, control.

using the TBA method, and the results revealed that the levels of MDA were markedly enhanced in the 6, 12 and 24 h groups, compared with that in the Con group (Fig. 1C). H&E staining was used to examine the changes in myocardial tissues, and it was found that myocardial fiber bundles were loosely arranged, some myocardial fibers were broken and dissolved, and some cardiomyocytes were degenerated and necrotic. Interstitial edema was noted and moderate inflammatory cell infiltration was observed as LPS processing time was prolonged (Fig. 1D).

Protein levels of cleaved caspase-1 are upregulated and strong staining for TXNIP and NLRP3 is present in sepsis-induced myocardial injury rats. In view of the importance of the TXNIP/NLRP3 signaling pathway in the development of sepsis-induced myocardial injury, the expression levels of cleaved caspase-1, caspase-1, TXNIP and NLRP3 were determined by western blot analysis or immunohistochemistry. It was found that the levels of cleaved caspase-1 were higher in the 6, 12 and 24 h groups compared with that in the Con group (Fig. 2A and B), and the intensity of staining of the rat myocardial sections treated with LPS was observed in a time-dependent manner (Fig. 2C).

Levels of IL-1β, IL-18, cleaved caspase-1, TXNIP and NLRP3 are significantly increased by LPS in H9C2 cells. In order to elucidate the mechanisms of sepsis-induced myocardial dysfunction, H9C2 cells were used to establish a model of sepsis-induced myocardial dysfunction using LPS (1, 10, 20 and 50 μg/ml) *in vitro*. The viability of cells was suppressed by LPS at 20 and 50 μg/ml (Fig. 3A). The mRNA levels of IL-1β, IL-18 (Fig. 3B) and TXNIP (Fig. 3C) were enhanced by LPS, and the protein levels of cleaved caspase-1, TXNIP and NLRP3 were also increased by LPS (Fig. 3D and E).

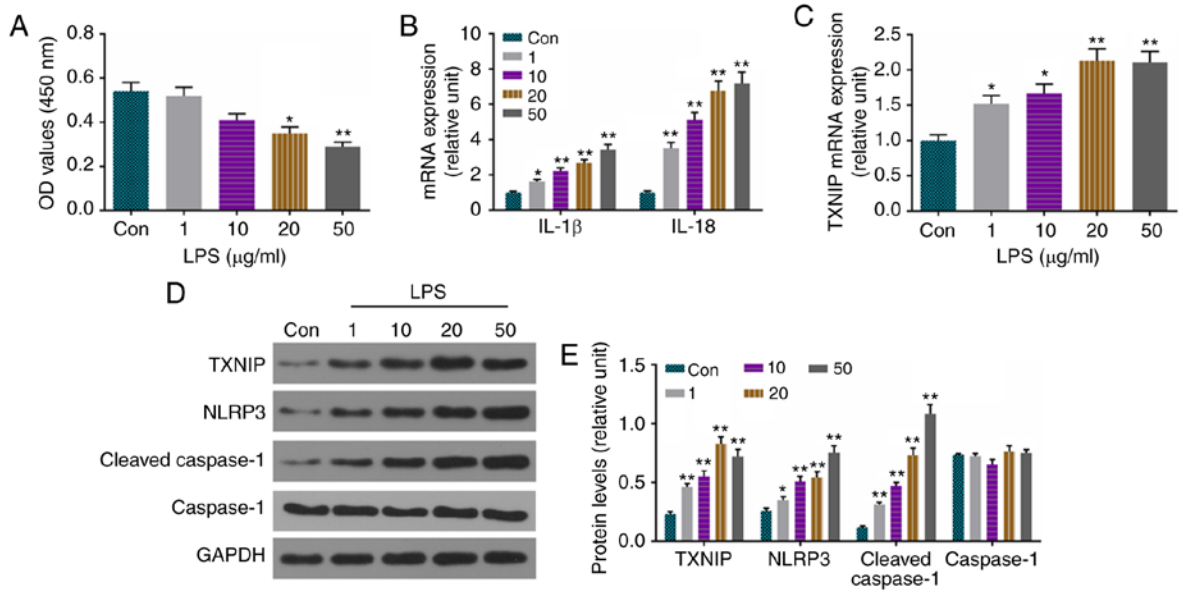

Figure 3. Levels of IL-1β, IL-18, cleaved caspase-1, TXNIP and NLRP3 are significantly increased by LPS in H9C2 cells. (A) Viability of cells was detected using a cell counting kit-8. (B) RT-qPCR analysis was used to detect the mRNA levels of IL-1β and IL-18. (C) mRNA levels of TXNIP were measured by RT-qPCR analysis. (D) Protein levels of cleaved caspase-1, caspase-1, TXNIP and NLRP3 were assessed by western blotting. (E) Relative levels of proteins in were determined with GAPDH for normalization. *P<0.05 and **P<0.01 vs. Con. IL, interleukin; TXNIP, thioredoxin-interacting protein; NLRP3, NOD-like receptor pyrin domain containing 3; LPS, lipopolysaccharide; Con, control; RT-qPCR, reverse transcription-quantitative polymerase chain reaction.

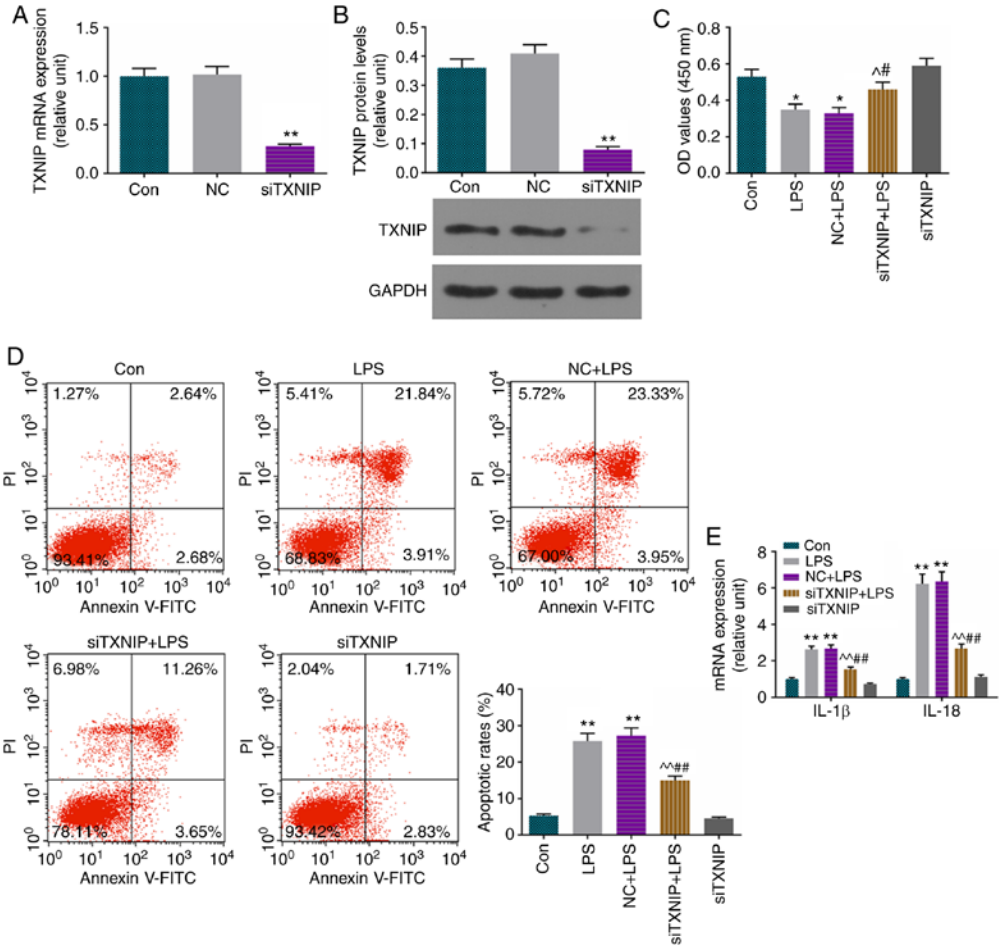

Figure 4. Apoptosis is increased and levels of IL-1β and IL-18 are increased by LPS, which is partially reversed by siTXNIP. Transfection efficiency of siTXNIP was assessed by (A) RT-qPCR and (B) western blot analyses. (C) Viability of cells was detected using a cell counting kit-8. (D) Apoptosis was quantified by flow cytometry. (E) RT-qPCR analysis was used to detect the mRNA levels of IL-1β and IL-18. *P<0.05 and **P<0.01 vs. Con; $^{\wedge}$P<0.05 and $^{\wedge\wedge}$P<0.01 vs. LPS; $^{\#}$P<0.05 and $^{\#\#}$P<0.01 vs. NC+LPS. TXNIP, thioredoxin-interacting protein; IL, interleukin; siTXNIP, small interfering RNA targeting TXNIP; LPS, lipopolysaccharide; NC, negative control; Con, control; RT-qPCR, reverse transcription-quantitative polymerase chain reaction.

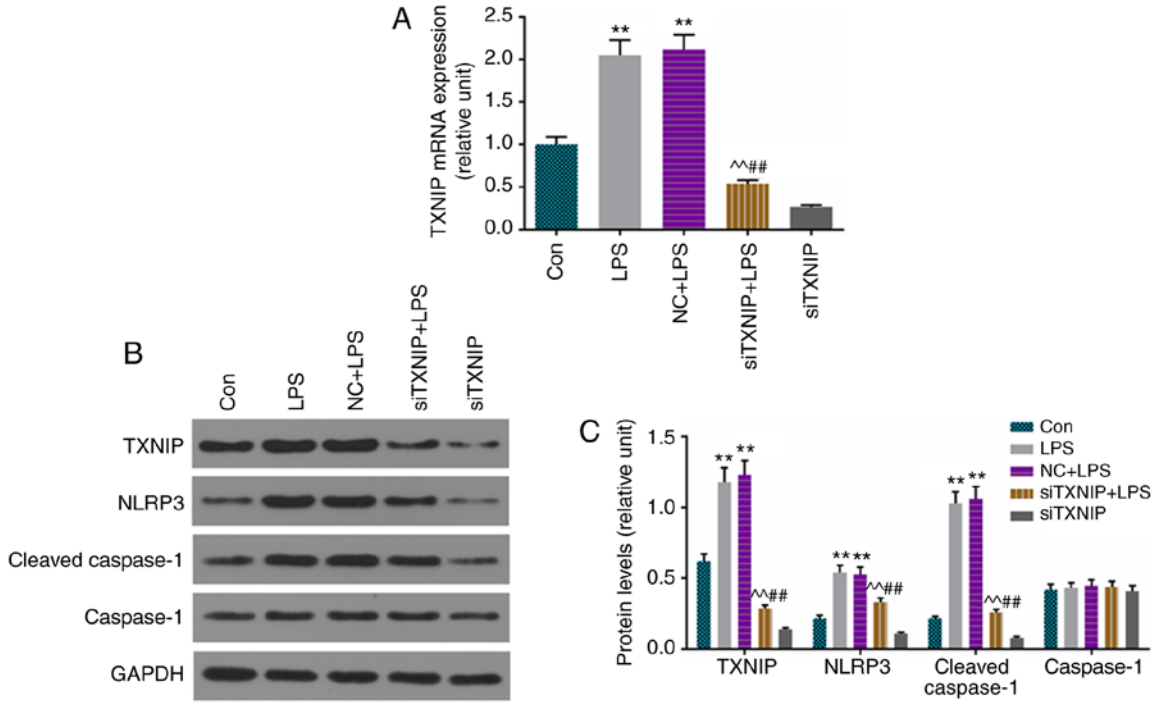

Figure 5. Improvements in cleaved caspase-1, TXNIP and NLRP3 are inhibited by siTXNIP. (A) Reverse transcription-quantitative polymerase chain reaction analysis was used to detect the mRNA levels TXNIP. (B) Protein levels of cleaved caspase-1, caspase-1, TXNIP and NLRP3 were assessed by western blotting. (C) Relative levels of proteins described were determined with GAPDH for normalization. **P<0.01 vs. Con; $^{\wedge\wedge}$P<0.01 vs. LPS; $^{\#\#}$P<0.01 vs. NC+LPS. TXNIP, thioredoxin-interacting protein; NLRP3, NOD-like receptor pyrin domain containing 3; IL, interleukin; siTXNIP, small interfering RNA targeting TXNIP; NC, negative control; LPS, lipopolysaccharide; Con, control.

Apoptosis is increased and levels of IL-1β and IL-18 are improved by LPS, and partially reversed by siTXNIP. To verify the role of TXNIP in the H9C2 cell model of sepsis-induced myocardial dysfunction, which was established using LPS (20 μg/ml), the TXNIP gene was knocked down by siRNA. Successful transfection using LFN was observed for TXNIP at the mRNA (Fig. 4A) and protein (Fig. 4B) levels. The viability of cells was decreased by LPS and ameliorated by siTXNIP (Fig. 4C). It was also found that the increase of apoptosis (Fig. 4D) and augmentation of IL-1β and IL-18 (Fig. 4E) were inhibited by siTXNIP in the LPS group.

Increases in expression of cleaved caspase-1, TXNIP and NLRP3 are repressed by siTXNIP. The levels of cleaved caspase-1, TXNIP and NLRP3 were determined by RT-qPCR or/and western blot analysis, and the results demonstrated that the mRNA level of TXNIP was lower in the siTXNIP+LPS group than in the LPS and NC+LPS groups (Fig. 5A), and that the protein levels of cleaved caspase-1, TXNIP and NLRP3 were inhibited by siTXNIP, compared with levels in the LPS and NC+LPS groups, respectively (Fig. 5B and C).

ROS production is elevated by LPS, which is partially reversed by siTXNIP. ROS levels were assessed by flow cytometry, and catalase and MnSOD were detected by RT-qPCR and western blot analyses. The results showed that ROS production was lower in the siTXNIP+LPS group than in the LPS and NC+LPS groups (Fig. 6A), and the levels of catalase and MnSOD were enhanced by siTXNIP, compared with levels in the LPS and NC+LPS groups at the mRNA (Fig. 6B) and protein (Fig. 6C and D) levels.

Discussion

Sepsis, which is a common complication of severe trauma, infection, shock and other stress states, has high incidence and high mortality rates (17). Sepsis-associated mortality is closely associated with damage, which can easily lead to multiple organ dysfunction, particularly heart damage (18). Therefore, it is necessary to examine the pathological mechanism of sepsis-induced myocardial injury in order to identify an effective therapeutic target.

LPS, which serves an important role in Gram-negative bacterial infection and disease evolution, is considered to be a main cause to systemic inflammatory syndrome (19). Sepsis-induced myocardial injury is one of the manifestations of multiple organ dysfunctions in sepsis, which has been confirmed in clinical and sepsis animal experiments (20). LPS is an important substance causing myocardial damage, which forces the contractile function in the body to weaken and heart rate to slow down, which seriously affects heart function (21). Afulukwe *et al* (22) found that intravenous injection of LPS (10 mg/kg) helped to prepare an SD rat septic shock model and create myocardial contractility, myocardial damage; the feasibility of such a model was confirmed by Cohen *et al* (23), Iqbal *et al* (21) and others. Following the intraperitoneal injection of LPS (l0 mg/kg) in Wistar rats, Chagnon *et al* (24) observed a decrease in left ventricular ejection fraction, which was consistent with the findings observed in patients with severe sepsis. Similarly, an animal model of sepsis was prepared by intraperitoneal injection of LPS (10 mg/kg) into SD rats, and the results showed that CTnT in the serum increased gradually as time progressed in the 6 h following LPS injection. CTnT

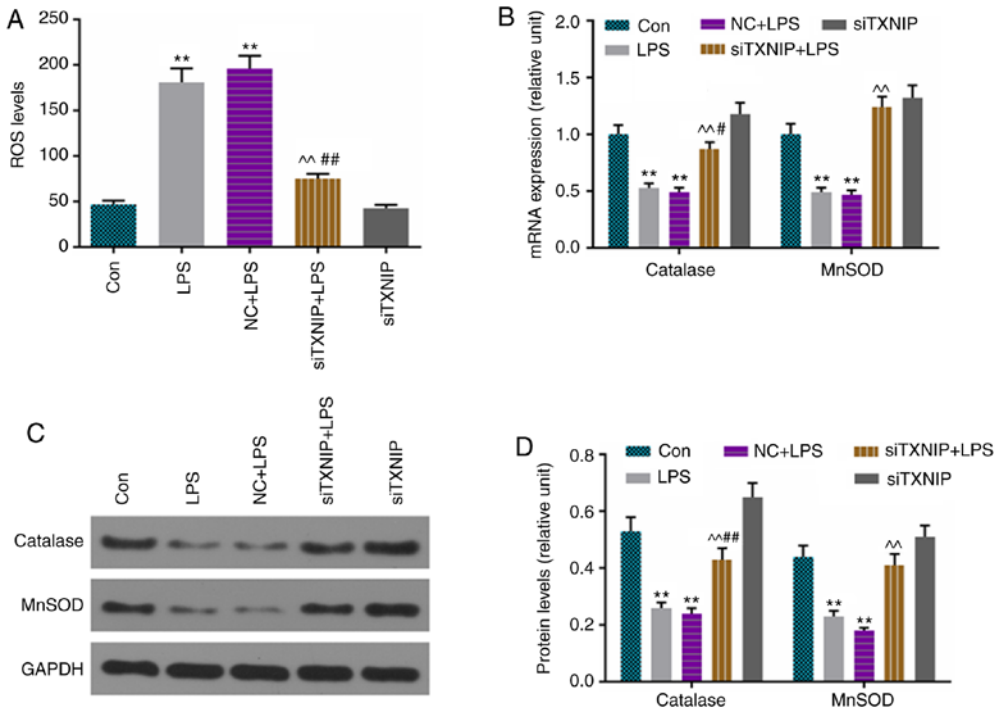

Figure 6. ROS production is elevated by LPS, which is partially reversed by siTXNIP. (A) ROS production was measured by flow cytometry. (B) Reverse transcription-quantitative polymerase chain reaction analysis was used to detect the mRNA levels of catalase and MnSOD. (C) Protein levels of catalase and MnSOD were assessed by western blotting. (D) Relative levels of proteins were determined with GAPDH for normalization. **P<0.01 vs. Con; $^{\wedge\wedge}$P<0.01 vs. LPS; $^{\#}$P<0.05 and $^{\#\#}$P<0.01 vs. NC+LPS. ROS, reactive oxygen species; TXNIP, thioredoxin-interacting protein; siTXNIP, small interfering RNA targeting TXNIP; MnSOD, manganese-superoxide dismutase; NC, negative control; LPS, lipopolysaccharide; Con, control.

is a sensitive indicator of myocardial damage (25). In patients with septic shock, elevated serum CTnT predicts a higher mortality rate and poor prognosis (26). In the present study, it was found that myocardial tissue in sepsis rats exhibited myocardial fiber rupture and lysis, cardiomyocyte eosinophilic changes, mild edema and inflammatory cell infiltration under a light microscope. As the treatment duration was prolonged, the above effects gradually became more marked. Some myocardial tissue necrosis was observed 24 h following LPS injection, and damage to myocardial fibers and mitochondrial ultrastructure were observed under an electron microscope. Therefore, it is feasible to prepare an animal model of myocardial injury in sepsis by intraperitoneal injection of 10 mg/kg LPS into SD rats. However, its underlying mechanisms remain to be fully elucidated.

Previous studies have shown that NLRP3 inflammatory bodies serve a key role in sepsis-induced myocardial injury (27-29) and the progression of acute inflammation (30). As its core protein, NLRP3 acts as a signal receptor in the cytoplasm, once activated, NLRP3 recruits ASC and caspase-1 and activates caspase-1 by the cleavage of IL-1β and IL-18 precursors, which mature and are secreted outside the cell and are involved in the inflammatory response (31). Yang *et al* found that the expression levels of NLRP3 and caspase-1 were increased in myocardial tissue treated with cecal ligation and puncture (27). IL-1β increases *in vivo* and *in vitro* in sepsis and septic shock (32,33). Cardiac contractile function is preserved and infarct size is reduced in mice deficient in components of the inflammasome complex (NLRP3) (34). Consistent with previous studies, the present study performed a systematic assessment of this pathway in sepsis-induced myocardial dysfunction *in vivo* and *in vitro*. The results showed that the expression levels of NLRP3, cleaved caspase-1, IL-1β and IL-18 were all significantly upregulated in sepsis-induced myocardial dysfunction *in vivo* and *in vitro*. These results demonstrated that the NLRP3 inflammasome serves a key role in the progression of sepsis-induced myocardial dysfunction.

Endotoxins, uric acid and ROS, which are activators of the NLRP3 inflammasome, have already been identified (35). TXNIP is a key antioxidant in the human body and is necessary for activation of the NLRP3 inflammasome via direct interaction with NLRP3 (36). Liu *et al* found that TXNIP and NLRP3 were significantly increased during myocardial ischemia/reperfusion injury and that siTXNIP significantly decreased activation of the NLRP3 inflammasome (37). The role of the TXNIP/NLRP3 signaling pathway in myocardial injury has been reported previously, however, it has not been reported in sepsis-induced myocardial dysfunction. In the present study, it was found that the levels of TXNIP were improved in sepsis-induced myocardial dysfunction *in vivo* and *in vitro*, and that ROS production was also increased *in vitro*, which was evident by decreases in catalase and MnSOD. To further examine the role of TXNIP in sepsis-induced myocardial dysfunction, siTXNIP was transfected into H9C2 cells. The data indicated that activation of NLRP3 was inhibited and ROS production was repressed by siTXNIP, accompanied by decreased IL-1β and IL-18 levels and increased catalase and MnSOD levels, respectively. Cell viability was improved and apoptosis was inhibited in the siTXNIP group, compared with that in the LPS and NC+LPS groups. These results showed that TXNIP is essential in the activation of the NLRP3 inflammasome in sepsis-induced myocardial dysfunction.

In conclusion, the results of the present study demonstrated that the NLRP3 inflammasome was activated in sepsis-induced myocardial dysfunction. Additionally, TXNIP was shown, for the first time, to mediate the activation of NLRP3 inflammasomes in H9C2 cells treated with LPS. siTXNIP inhibited activation of the NLRP3 inflammasome, and such a result may provide novel therapies for mitigating sepsis-induced myocardial dysfunction.

Acknowledgements

Not applicable.

Funding

This study was supported by the Zhejiang Provincial Medicine and Health Research Foundation (grant no. 2019KY002).

Availability of data and materials

The analyzed datasets generated during this study are available from the corresponding author on reasonable request.

Authors' contributions

CY made substantial contributions to conception and design; WX and XL performed data acquisition, data analysis and interpretation; JL contributed to drafting and critical revision of the manuscript for important intellectual content; all authors approved the final version to be published; AW and CY agreed to be accountable for all aspects of the work in ensuring that questions related to the accuracy or integrity of the work were appropriately investigated and resolved. All authors read and approved the final manuscript.

Ethics approval and consent to participate

All animal protocols were approved by Zhejiang University Animal Committee (Zhejiang, China).

Patient consent for publication

Not applicable.

Competing interests

The authors declare that they have no competing interests.

References

1. Xu YB ZH, Chen SZ, Chen GR and Guo S: Optimization and identification of anti-sepsis potential targets of palmatine. Chin J Mod Appl Pharm 35: 1602-1605, 2018.
2. Stanzani G, Duchen MR and Singer M: The role of mitochondria in sepsis-induced cardiomyopathy. Biochim Biophys Acta Mol Basis Dis 1865: 759-773, 2019.
3. Rabuel C and Mebazaa A: Septic shock: A heart story since the 1960s. Intensive Care Med 32: 799-807, 2006.
4. Rudiger A and Singer M: Mechanisms of sepsis-induced cardiac dysfunction. Crit Care Med 35: 1599-1608, 2007.
5. Meng F, Lai H, Luo Z, Liu Y, Huang X, Chen J, Liu B, Guo Y, Cai Y and Huang Q: Effect of xuefu zhuyu decoction pretreatment on myocardium in sepsis rats. Evid Based Complement Alternat Med 2018: 2939307, 2018.
6. Anthonymuthu TS, Kim-Campbell N and Bayir H: Oxidative lipidomics: Applications in critical care. Curr Opin Crit Care 23: 251-256, 2017.
7. Al-Salam S and Hashmi S: Myocardial ischemia reperfusion injury: Apoptotic, inflammatory and oxidative stress role of galectin-3. Cell Physiol Biochem 50: 1123-1139, 2018.
8. Su Q, Li L, Sun Y, Yang H, Ye Z and Zhao J: Effects of the TLR4/Myd88/NF-κB signaling pathway on NLRP3 inflammasome in coronary microembolization-induced myocardial injury. Cell Physiol Biochem 47: 1497-1508, 2018.
9. Kayagaki N, Stowe IB, Lee BL, O'Rourke K, Anderson K, Warming S, Cuellar T, Haley B, Roose-Girma M, Phung QT, *et al*: Caspase-11 cleaves gasdermin D for non-canonical inflammasome signalling. Nature 526: 666-671, 2015.
10. Chen W, Zhao M, Zhao S, Lu Q, Ni L, Zou C, Lu L, Xu X, Guan H, Zheng Z and Qiu Q: Activation of the TXNIP/NLRP3 inflammasome pathway contributes to inflammation in diabetic retinopathy: A novel inhibitory effect of minocycline. Inflamm Res 66: 157-166, 2017.
11. Zheng R, Tao L, Jian H, Chang Y, Cheng Y, Feng Y and Zhang H: NLRP3 inflammasome activation and lung fibrosis caused by airborne fine particulate matter. Ecotoxicol Environ Saf 163: 612-619, 2018.
12. Takimoto E and Kass DA: Role of oxidative stress in cardiac hypertrophy and remodeling. Hypertension 49: 241-248, 2007.
13. Haileselassie B, Su E, Pozios I, Niño DF, Liu H, Lu DY, Ventoulis I, Fulton WB, Sodhi CP, Hackam D, *et al*: Myocardial oxidative stress correlates with left ventricular dysfunction on strain echocardiography in a rodent model of sepsis. Intensive Care Med Exp 5: 21, 2017.
14. Assem M, Teyssier JR, Benderitter M, Terrand J, Laubriet A, Javouhey A, David M and Rochette L: Pattern of superoxide dismutase enzymatic activity and RNA changes in rat heart ventricles after myocardial infarction. Am J Pathol 151: 549-555, 1997.
15. Lone MU, Baghel KS, Kanchan RK, Shrivastava R, Malik SA, Tewari BN, Tripathi C, Negi MP, Garg VK, Sharma M, *et al*: Physical interaction of estrogen receptor with MnSOD: Implication in mitochondrial $O2^{\cdot-}$ upregulation and mTORC2 potentiation in estrogen-responsive breast cancer cells. Oncogene 36: 1829-1839, 2017.
16. Livak KJ and Schmittgen TD: Analysis of relative gene expression data using real-time quantitative PCR and the 2(-Delta Delta C(T)) method. Methods 25: 402-408, 2001.
17. Klingenberg C, Kornelisse RF, Buonocore G, Maier RF and Stocker M: Culture-negative early-onset neonatal sepsis-at the crossroad between efficient sepsis care and antimicrobial stewardship. Front Pediatr 6: 285, 2018.
18. Liu H, Sun Y, Zhang Y, Yang G, Guo L, Zhao Y and Pei Z: Role of thymoquinone in cardiac damage caused by sepsis from BALB/c mice. Inflammation 42: 516-525, 2019.
19. Stoll LL, Denning GM and Weintraub NL: Potential role of endotoxin as a proinflammatory mediator of atherosclerosis. Arterioscler Thromb Vasc Biol 24: 2227-2236, 2004.
20. Kakihana Y, Ito T, Nakahara M, Yamaguchi K and Yasuda T: Sepsis-induced myocardial dysfunction: Pathophysiology and management. J Intensive Care 4: 22, 2016.
21. Iqbal M, Cohen RI, Marzouk K and Liu SF: Time course of nitric oxide, peroxynitrite, and antioxidants in the endotoxemic heart. Crit Care Med 30: 1291-1296, 2002.
22. Afulukwe IF, Cohen RI, Zeballos GA, Iqbal M and Scharf SM: Selective NOS inhibition restores myocardial contractility in endotoxemic rats; however, myocardial NO content does not correlate with myocardial dysfunction. Am J Respir Crit Care Med 162: 21-26, 2000.
23. Cohen RI, Wilson D and Liu SF: Nitric oxide modifies the sarcoplasmic reticular calcium release channel in endotoxemia by both guanosine-3',5' (cyclic) phosphate-dependent and independent pathways. Crit Care Med 34: 173-181, 2006.
24. Chagnon F, Bentourkia M, Lecomte R, Lessard M and Lesur O: Endotoxin-induced heart dysfunction in rats: Assessment of myocardial perfusion and permeability and the role of fluid resuscitation. Crit Care Med 34: 127-133, 2006.
25. Maxwell MH, Robertson GW and Moseley D: Potential role of serum troponin T in cardiomyocyte injury in the broiler ascites syndrome. Br Poult Sci 35: 663-667, 1994.
26. Choon-ngarm T and Partpisanu P: Serum cardiac troponin-T as a prognostic marker in septic shock. J Med Assoc Thai 91: 1818-1821, 2008.

27. Yang L, Zhang H and Chen P: Sulfur dioxide attenuates sepsis-induced cardiac dysfunction via inhibition of NLRP3 inflammasome activation in rats. Nitric Oxide 81: 11-20, 2018.
28. Wu D, Shi L, Li P, Ni X, Zhang J, Zhu Q, Qi Y and Wang B: Intermedin1-53 protects cardiac fibroblasts by inhibiting NLRP3 inflammasome activation during sepsis. Inflammation 41: 505-514, 2018.
29. Zhang B, Liu Y, Sui YB, Cai HQ, Liu WX, Zhu M and Yin XH: Cortistatin inhibits NLRP3 inflammasome activation of cardiac fibroblasts during sepsis. J Card Fail 21: 426-433, 2015.
30. Lopes de Oliveira GA, Alarcón de la Lastra C, Rosillo MÁ, Castejon Martinez ML, Sánchez-Hidalgo M, Rolim Medeiros JV and Villegas I: Preventive effect of bergenin against the development of TNBS-induced acute colitis in rats is associated with inflammatory mediators inhibition and NLRP3/ASC inflammasome signaling pathways. Chem Biol Interact 297: 25-33, 2019.
31. Shen HH, Yang YX, Meng X, Luo XY, Li XM, Shuai ZW, Ye DQ and Pan HF: NLRP3: A promising therapeutic target for autoimmune diseases. Autoimmun Rev 17: 694-702, 2018.
32. Clavier T, Besnier E, Lefevre-Scelles A, Lanfray D, Masmoudi O, Pelletier G, Castel H, Tonon MC and Compère V: Increased hypothalamic levels of endozepines, endogenous ligands of benzodiazepine receptors, in a rat model of sepsis. Shock 45: 653-659, 2016.
33. Hara Y, Shimomura Y, Nakamura T, Kuriyama N, Yamashita C, Kato Y, Miyasho T, Sakai T, Yamada S, Moriyama K and Nishida O: Novel blood purification system for regulating excessive immune reactions in severe sepsis and septic shock: An ex vivo pilot study. Ther Apher Dial 19: 308-315, 2015.
34. Sandanger Ø, Ranheim T, Vinge LE, Bliksøen M, Alfsnes K, Finsen AV, Dahl CP, Askevold ET, Florholmen G, Christensen G, *et al*: The NLRP3 inflammasome is up-regulated in cardiac fibroblasts and mediates myocardial ischaemia-reperfusion injury. Cardiovasc Res 99: 164-174, 2013.
35. Jin C and Flavell RA: Molecular mechanism of NLRP3 inflammasome activation. J Clin Immunol 30: 628-631, 2010.
36. Nishiyama A, Matsui M, Iwata S, Hirota K, Masutani H, Nakamura H, Takagi Y, Sono H, Gon Y and Yodoi J: Identification of thioredoxin-binding protein-2/vitamin D(3) up-regulated protein 1 as a negative regulator of thioredoxin function and expression. J Biol Chem 274: 21645-21650, 1999.
37. Liu Y, Lian K, Zhang L, Wang R, Yi F, Gao C, Xin C, Zhu D, Li Y, Yan W, *et al*: TXNIP mediates NLRP3 inflammasome activation in cardiac microvascular endothelial cells as a novel mechanism in myocardial ischemia/reperfusion injury. Basic Res Cardiol 109: 415, 2014.

This work is licensed under a Creative Commons Attribution-NonCommercial-NoDerivatives 4.0 International (CC BY-NC-ND 4.0) License.